

## Damage states of cut-and-cover tunnels under seismic excitation

Duhee Park<sup>1</sup>, Tae-Hyung Lee<sup>2</sup>, Jin-Man Kim<sup>3</sup>

### ABSTRACT

We identify the damage states of single-barrel rectangular cut-and-cover tunnels under seismic loading from inelastic frame analyses using nonlinear models for steel and concrete. The pattern of propagation of plastic hinges in the reinforced concrete lining is observed. Based on the plastic hinges that are generated in the tunnel, four damage states are identified. We relate the damage state with equivalent maximum moment calculated from linear frame analyses normalized to the resisting moment. We also relate the damage state with free field shear strain and shear wave velocity.

### Introduction

The construction of metro systems in large urban areas is important for socioeconomic development of a modern country. The underground space plays important roles in the transportation network of a city. In general, underground structures were shown to suffer less damage than above-ground structures during seismic events. However, it was demonstrated that even underground structures can be vulnerable under strong seismic excitations, including the 1999 Chi-Chi, Taiwan earthquake, the 2004 Mid Niigata Prefecture, Japan earthquake and the 2008 Wenchuan, China earthquake (Wang and Zhang, 2013; Hashash et al., 2001).

Underground structures embedded in soil layers or rock and primarily subjected by the deformation of the surrounding ground, therefore their behavior have distinct differences compared to superstructures under an earthquake event (Wood, 2004). Even though the tunnel is expected to undergo inelastic behavior under severe earthquake event, previous studies assumed that the tunnel behaves linear elastically even close to collapse (Wang, 1993; Hashash et al., 2001; Argyroudis and Pitilakis, 2012). Fragility curves of rectangular structures have been proposed, assuming linear elastic response of tunnels (Argyroudis and Pitilakis, 2012; Androtti and Martinelli, 2013). However, the accuracy of such an assumption has not been thoroughly investigated.

We investigate the non-linear behavior of rectangular cut-and-cover tunnels under seismic loading from inelastic reinforced concrete frame analysis. The deformation of the ground is imposed to the springs connected to the tunnel frame as displacement boundary conditions. We

---

<sup>1</sup> Associate professor, Department of Civil and Environmental Engineering, Hanyang University, Seoul, Korea, [dpark@hanyang.ac.kr](mailto:dpark@hanyang.ac.kr)

<sup>2</sup> Associate professor, Department of Civil and Environmental Engineering, Konkuk University, Seoul, Korea, [thlee@konkuk.ac.kr](mailto:thlee@konkuk.ac.kr)

<sup>3</sup> Professor, Department of Civil and Environmental Engineering, Pusan National University, Seoul, Korea, [jmkim@pusan.ac.kr](mailto:jmkim@pusan.ac.kr)

also applied shear stress induced by the deformation of the ground to the tunnel structural elements. Response of the tunnel from elastic to inelastic range and the development and propagation of plastic hinges are observed. Based on the analysis results, representative shear strain ranges at which the plastic hinges develop are identified.

### Numerical simulations

The cut-and-cover tunnels used in the numerical simulation are shown in Figure 1. We modeled two types of tunnels, which are single-barrel and double-barrel type tunnels, as shown in Figure 1a and b, respectively. Both are actual tunnels built in Korea. Same soil profile, which was assumed to be uniform and has a soil cover of 7 m, was used for both tunnels. The structural details of the tunnel sections are shown in Figure 2. The dimension of the outer sections A-A, B-B, and C-C are identical, but differ in reinforced steels used. It should be noted that the inner column of double-barrel tunnel, section D-D, has the smallest dimension.

The elastic modulus (E) and shear modulus (G) of concrete used were  $2.48 \times 10^7 \text{ kN/m}^2$  and  $1.03 \times 10^7 \text{ kN/m}^2$ , respectively, while for steel they were  $2 \times 10^8 \text{ kN/m}^2$  and  $7.7 \times 10^7 \text{ kN/m}^2$ , respectively. The specified concrete compressive strength ( $f_c'$ ) used was  $2.75 \times 10^4 \text{ kN/m}^2$  and the yield stress ( $f_y$ ) of longitudinal steel was assumed as  $4.13 \times 10^5 \text{ kN/m}^2$ . Nonlinear models were used for the concrete and reinforced steel bars, as shown in Figure 3. Moment-curvature relationship of section A-A computed from section analysis using SAP2000 is shown in Figure 4.

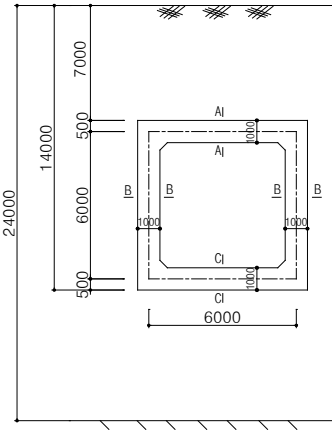


Figure 1. Soil profile and tunnel dimensions: (a) single-barrel tunnel (b) double-barrel tunnel

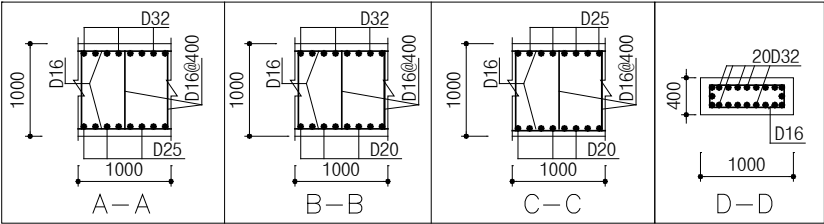


Figure 2. Sectional details of the tunnel

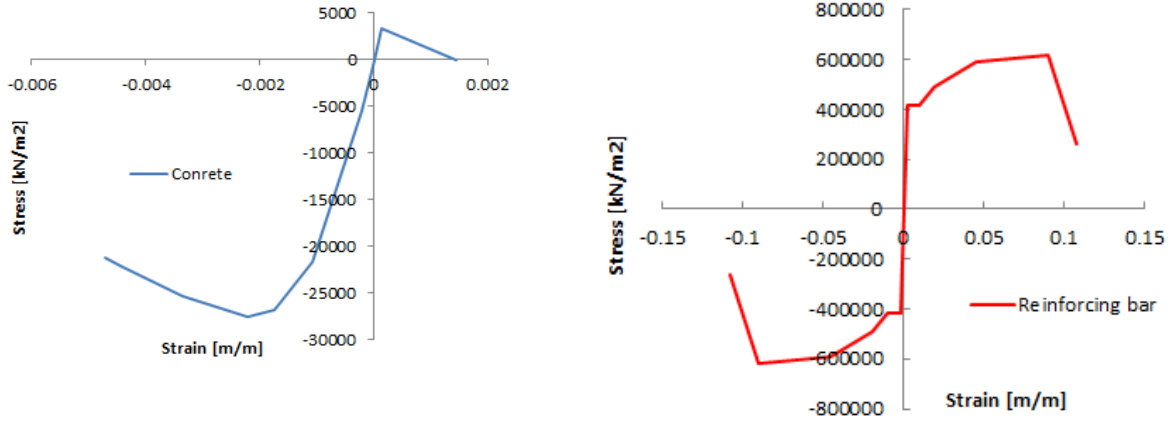


Figure 3. Numerical models for concrete and reinforced steel

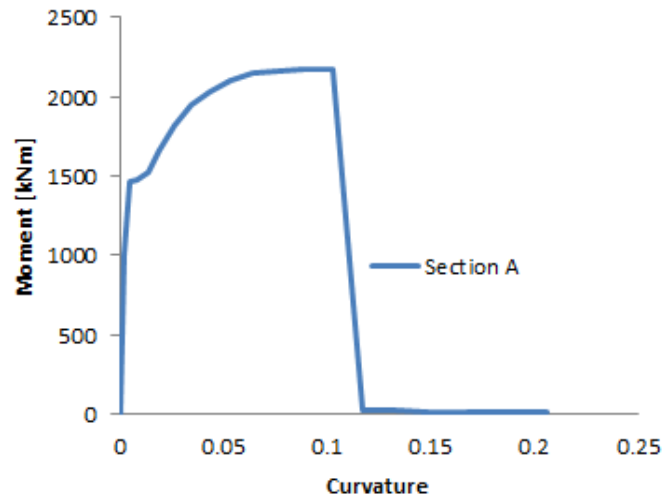


Figure 4. Moment-curvature curve of section A-A

Numerical simulations were performed using SAP2000 software. The schematic plot of the tunnel frame model and applied geostatic forces and seismically induced displacement is shown in Fig. 4. Each structural element of the models is divided into 64 small elements and the offsets at the corners of tunnels were also modeled. The frame hinge type for the concrete beam is applied for all elements [FEMA 356, 2000]. This implementation indicates that plastic hinges can occur anywhere in the frame elements of the structure.

The coefficient of horizontal and vertical subgrade reactions are respectively defined as  $K_H = k_{h0} \left( \frac{h}{30} \right)^{-3/4}$  and  $K_V = k_{h0} \left( \frac{b}{30} \right)^{-3/4}$  where  $k_{h0} = \left( \frac{1}{30} \right) E_D$ ,  $h$  and  $b$  are respectively the height and the width of the tunnel wall,  $E_D$  is dynamic elastic modulus  $E_D = 2(1 + \nu_D)G_D$ ,  $\nu_D$  is dynamic Poisson's ratio of soil,  $G_D$  is dynamic shear modulus calculated as  $G_D = (\gamma_t/g)E_s^2$ ,  $\gamma_t$  is the density of soil,  $V_s$  is the shear velocity of surrounding soil and  $g$  is the gravitational acceleration.

We performed push over analyses until the tunnel reaches failure. The schematic plot of the analysis is shown in Fig. 4. Five shear wave velocities were used to investigate the effect of the stiffness of the soil. Firstly, the geostatic stresses were applied to the vertical and lateral boundaries. The coefficient of lateral earth pressure ( $K_o$ ) was set to 0.5. Secondly, we applied displacement to the springs at the lateral boundaries and also to the shear springs at the top of the slab. We also applied shear stresses directly to the structural elements. The development of plastic hinges within the tunnel structural elements was observed and the moment and base forces were calculated. It should be noted that we did not account for the nonlinear behavior of soil. To use the numerical model, representative shear strain and corresponding reduced shear modulus ( $V_s$ ) determined from a site response analysis are needed. The nonlinear soil behavior may also influence the development of hinges, due to change in the stiffness with shearing, but it is not modeled this study. In addition, it should be noted that we did not account for the effect of the construction method of the tunnel. Possible changes in the soil properties between the original ground and backfilled soil covering the cut-and-cover tunnel were ignored.

### Results of simulation

Fig. 5 shows the results of the pushover analysis. The base shear force is plotted against the top horizontal displacement for single barrel rectangular structures in soils ranging in shear wave velocities from 50 m/s to 400 m/s. The base shear is significantly lower for low shear velocity soils, demonstrating that a much higher shear deformation is required for softer soils to reach the same level of base shear. Fig. 6 displays the moments calculated in the structural elements against free field shear strain. It is shown that the shear strain at which the plastic hinges form depend greatly on the stiffness of the soil.

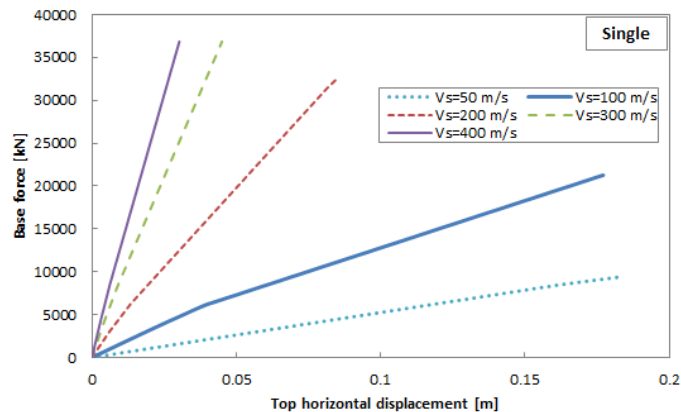


Figure 5. Pushover curves for the single barrel tunnel

The sequences and the positions of the plastic hinges of the single box are illustrated in Fig. 7 - 8. The relative displacement shown in the figure is the difference in the horizontal displacement between the top and bottom slabs divided by the height of the tunnel. It is equivalent to the induced shear strain in the soil. The first plastic hinge develops at the left bottom corner, followed by the right bottom corner. Third hinge develops at the right top corner, positioned diagonally from the first plastic hinge. The fourth and final plastic hinge develops at the top left

corner. It is shown that the bottom corners are more susceptible to seismic damage than the top corners. For  $V_s = 50$  m/sec, first plastic hinge forms at a high shear strain of 1.2%. The tunnel collapses when the shear strain is as high as 2.5%. It is demonstrated that a very high level of shear strain is needed to cause collapse of the single barrel box tunnel. Fig 7 shows the sequence of plastic hinges and corresponding relative displacements for a box tunnel in a soil with  $V_s = 400$  m/s. The sequence of plastic hinges that develop within the structure is different from the case of  $V_s = 50$  m/s. After the first hinge develops in the left bottom corner, the second hinge is formed at the top right corner. Third and fourth hinges develop at the right bottom and top left corners, respectively. Also to be noted is the very low levels of shear strains at which the plastic hinges are formed. The first hinge develops at a low shear strain amplitude of 0.04 %. The tunnel collapses at a shear strain of 0.12 %. The calculations highlight that a severe structural damage will be induced in a box tunnel at very low levels of shear strain.

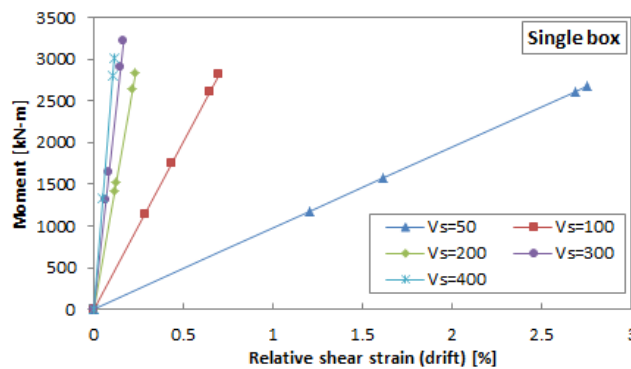


Figure 6. Moment versus relative shear strain (%) relationship at the formation of plastic hinges (shown as filled dots)

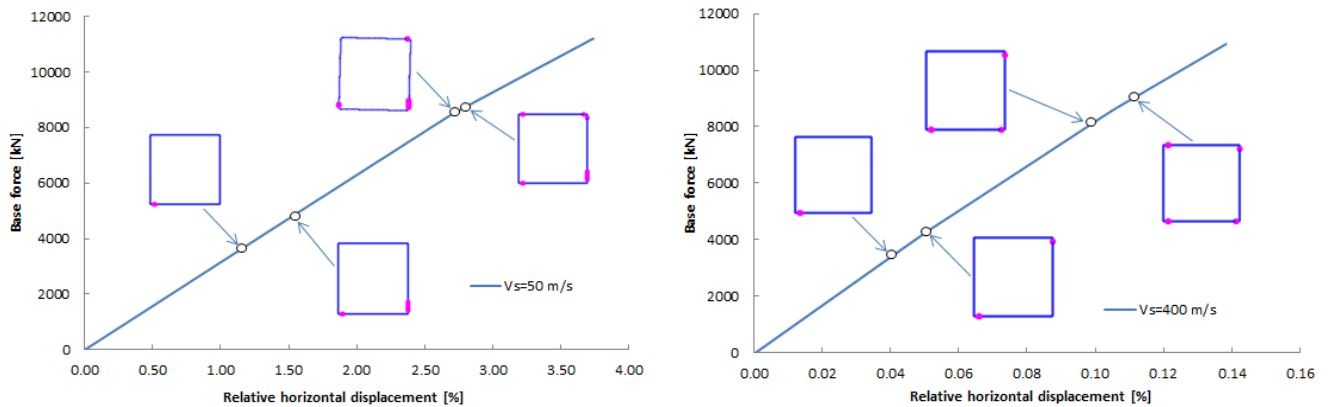


Fig. 7 Sequence of plastic hinges that develops in a single barrel box tunnel embedded in uniform soils with different shear wave velocities: a)  $V_s = 50$  m/s b)  $V_s = 400$  m/s

## Conclusions

A series of 2D inelastic frame analyses were performed to identify the collapse mechanism of frame tunnels under seismic loading. The dynamic response of box tunnels was represented via a pseudo-static analysis where the free-field deformation was imposed as displacement boundaries and shear stresses to the springs attached to the tunnel structure. The pattern of propagation of plastic hinges in the reinforced concrete lining was observed. It is shown that the plastic hinge start to form at the bottom corners of the structure. The shear strain at which the tunnel collapses are dependent of the shear wave velocity of the soil. Whereas the plastic hinge develops at a shear strain of 1.2 % for soils with a shear velocity of 50 m/s, it is formed at a low shear strain of 0.04 %. The shear strain – moment diagram proposed in this study provide a simple yet robust method to evaluate the seismic performance of cut-and-cover box tunnels under seismic loading.

## Acknowledgement

This research was supported by National Research Foundation of Korea Grant (2015R1A2A2A01006129).

## References

- Androtti G., Lai G.C, Martinelli M., 2013. Seismic fragility functions of deep tunnels: A new cumulative damage model based on lumped plasticity and rotation capacity. *ICEGE Istanbul*, Turkey.
- Argyroudis S.A, Pitilakis K.D., 2012. Seismic fragility curves of shallow tunnels in alluvial deposit, *Soil Dynamics and Earthquake Engineering* **35**, 1-12.
- FEMA 356, 2000. *Prestandard and Commentary for the Seismic Rehabilitation of Buildings*, ASCE.
- Hashash et al, 2001. Seismic design and analysis of underground structure. *Tunnel and Underground Space Technology* **16**, 247-293.
- K. Pitilakis and G. Tsiniadis, 2014. Chapter 11 Performance and Seismic Design of Underground Structures. *Earthquake Geotechnical Engineering Design*, Springer International Publishing Switzerland.
- S. Argyroudis and A.M. Kaynia, 2014. Fragility functions of Highway and Railway Infrastructure, Chapter 10 of *SYNER-G: Typology Definition and Fragility Functions for Physical Elements at Seismic Risk*, Springer Science+Business Media Dordrecht.
- Wang J.N, 1993. *Seismic Design of Tunnels*, A simple State-of-Art Design Approach.
- Wood J.H, 2004. *Earthquake design procedures for rectangular underground structures*. EQC Project No 01/470.
- Z.Z.Wang, Z. Zhang, 2013. Seismic damage classification and risk assessment of mountain tunnels with a validation for 2008 Wenchuan earthquake. *Soil Dynamic and Earthquake Engineering*, **45**, 45-55.